

Specific-heat measurements and critical exponents of the ferroelastic phase transition in $Pb_3(PO_4)_2$ and $Pb_3(P_{1-x}As_xO_4)_2$

E. Salje and B. Wruck

Institut für Kristallographie und Petrographie, Universität Hannover, Welfengarten 1, D-3000 Hannover 1, Federal Republic of Germany

(Received 15 October 1982; revised manuscript received 25 February 1983)

The ferroelastic phase transitions in $Pb_3(PO_4)_2$ and $Pb_3(P_{1-x}As_xO_4)_2$ are accompanied by large excess specific heats in a wide temperature range above T_c and critical crossover above and below T_c . Critical exponents of the specific heat $\alpha' = 0.363(4)$, $0.360(5)$, and $0.36(1)$ for $Pb_3(PO_4)_2$, $Pb_3(P_{0.97}As_{0.03}O_4)_2$, and $Pb_3(P_{0.2}As_{0.8}O_4)_2$, respectively, agree with theoretical predictions of a $q = 3$, $d = 2$, Potts model. Along with other experimental results of neutron and Raman scattering, the specific-heat behavior above T_c indicates dynamical fluctuations in $Pb_3(PO_4)_2$ and a static intermediate phase in the mixed crystals. A strict proportionality between the transition entropy ΔS and the spontaneous birefringence Δn_{bc} was observed in $Pb_3(PO_4)_2$ at temperatures up to 415 K. Nonlinear behavior was found close to the transition point (453.6 K), which is interpreted in terms of a multicomponent order-parameter theory.

I. INTRODUCTION

Lead phosphate, $Pb_3(PO_4)_2$, and the isostructural mixed crystals $Pb_3(P_{1-x}As_xO_4)_2$ possess ferroelastic transitions between a trigonal phase $R\bar{3}m$ and a monoclinic phase $C2/c$. This transition was, in the case of $Pb_3(PO_4)_2$, originally interpreted in a Landau formalism with tricritical behavior.¹ Bismayer *et al.*² determined the order-parameter exponent β from the spontaneous birefringence and observed a nearly tricritical value $\beta = 0.235 \pm 0.008$ for $Pb_3(PO_4)_2$ below $T_c - 20$ K. Between $T_c - 20$ K and T_c a first-order behavior was found. Wood *et al.*³ made a similar observation and interpreted the crossover at $T_c - 20$ K self-consistently in terms of a special temperature dependence of the fourth-order term in a single-order-parameter Landau functional. Recently, a multicomponent-order-parameter model has been developed by Salje and Devarajan⁴ which also explains the observed monoclinic domains in the paraelastic phase. It starts from the effective Hamiltonian of the n -component Landau-Ginzburg-Wilson (LGW) Hamiltonian

$$\begin{aligned} \Phi = & \frac{\alpha}{2}(Q_1^2 + Q_2^2) + \frac{\alpha'}{2}Q_3^2 + (Q_1^2 + Q_2^2)^2L_2 \\ & + Q_3^2(Q_1^2 + Q_2^2)L_3 + Q_3^4L_1 \\ & + \frac{1}{\sqrt{2}}Q_1Q_3(Q_3^2 - \frac{1}{3}Q_2^2)L_4, \end{aligned} \tag{1}$$

with coefficients defined in Ref. 4. A diagonalization is possible under the assumption of well-separated fixed points of $\{Q_1, Q_2\}$ and $\{Q_3\}$. The parameters Q_1 and Q_2 then describe the effective Hamiltonian of a Potts oscillator^{4,5}

$$\begin{aligned} \Phi'' = & \left[\frac{\alpha}{2} + L_3M^2 \right] (Q_1^2 + Q_2^2) + L_2(Q_1^2 + Q_2^2)^2 \\ & + wQ_1(Q_2^2 - \frac{1}{3}Q_1^2), \end{aligned} \tag{2}$$

so we expect that its critical exponents belong to the three-state Potts model.⁶ Structurally, the three states described by $\{Q_1, Q_2\}$ are represented by three possible orientations of the monoclinic crystallographic axes of the low-temperature phase ($C2/c$) with respect to the trigonal unit cell of the high-temperature phase ($R\bar{3}m$).^{2,7,8} The stepwise character of the phase transition is then due to two processes. First, far above the ferroelastic transition point T_c , three zone-boundary modes start to condense, giving rise to static shifts of the Pb positions from the ternary axis in three directions, which are still symmetrically equivalent. At T_c the parameters Q_1 and Q_2 become critical. They describe the respective occupation number of the three fixed points in the monoclinic b - c plane and the symmetry is broken from trigonal to monoclinic. Although the order-parameter behavior for $T \ll T_c$ is well known from various experiments^{2,3,7} no information exists for the behavior at $T \approx T_c$ and $T > T_c$.

In the present work the temperature dependence of the excess entropy ΔS is determined and related to the order parameters. This relation follows from Eq. (1):

$$\frac{d\Phi}{dT} = -\Delta S = \frac{\alpha_1}{2}(Q_1^2 + Q_2^2) + \frac{\alpha_2}{2}Q_3^2 \tag{3}$$

with $\alpha_1 = \partial\alpha/\partial T$ and $\alpha_2 = \partial\alpha'/\partial T$.

Using the results of differential scanning calorimetry, this paper attempts to answer the following questions.

- (1) What is the temperature dependence of the entropy ΔS ?
- (2) What is the behavior of the specific-heat singularity close to T_c for the different compositions?
- (3) Does a second transition point exist above T_c ?

II. EXPERIMENTAL

The crystals were grown from the melt by the Chochralski method.⁷ For the experiments thin plates were cut with a typical size of $4 \times 4 \times 0.5$ mm³. The largest surface was parallel to the cleavage plane (100)_{mon} and was perfectly even, so that good thermal contact during the measurements of the heat capacities was guaranteed. All samples were weighed to an accuracy of ± 0.002 mg by means of a Mettler Mikrowaage M5 balance. Typical samples were of order 60 mg mass. The heat capacities were measured using a Perkin-Elmer DSC-2C differential scanning calorimeter with a digital interface and a Tektronix Programmable Calculator TK-31. The measurements were made at a heating rate of 10 K/min and a range setting of 5 mJ/sec. The temperature calibration of the calorimeter was better than ± 0.1 K, checked by measuring the transition temperatures of indium, tin, and lead. The specific heats were determined using sapphire as a C_p reference standard.⁹ The C_p values for sapphire were taken from Ref. 10. Several measurements were made for overlapping temperature ranges with the same temperature interval (56 K). Finally, ten C_p values were measured independently for each temperature and the average C_p value was taken [Figs. 1(a), 1(b), and 1(c)]. The standard deviations of the mean values were always below 0.2%.

At temperatures $T < T_c$ an increase of the specific heat and a sharp peak at T_c due to the ferroelastic phase transition occur. In contrast to Gilletta *et al.*¹¹ we observed a second anomaly at temperatures $T > T_c$. There was a small break and a slight change in the slope at T_3 in all the C_p curves and additional small peaks at T_2 for samples containing As. The values of T_c , T_2 , and T_3 , and of the latent heat L , are given in Table I.

The excess entropy is calculated from the specific heat using the expression

$$-\Delta S = \frac{L}{T_c} + \int_T^{T_c} \frac{\Delta C_p}{T} dT, \quad (4)$$

where ΔC_p is the excess specific heat due to the structural phase transition. To obtain ΔC_p the background specific heat must be subtracted from the experimental values as shown in Fig. 1. The extrapolation of the background specific heat is based upon the empirical temperature

dependence of the form

$$C_p^0 = a + bT^{-1}. \quad (5)$$

The parameters a and b were determined by a least-squares fit of the experimental data for $T > T_3$. In the case of $\text{Pb}_3(\text{PO}_4)_2$ the resulting standard deviations are 0.24% for a and 1.4% for b , but larger for the mixed crystals. In this case a further fixed point was constructed at 370 K using the order-parameter dependence of ΔS in Eq. (3). The temperature dependence of the Q_i at $T \ll T_c$ is known from measurement of the spontaneous birefringence Δn_{bc} .⁷ In the limit of low temperature Δn_{bc} depends quadratically on the Q_i and we assume, therefore, a linear dependence between ΔS and Δn_{bc} . The value of C_p^0 at 370 K was chosen so that the ratio between ΔS (370 K) and L/T_c is the same as between Δn_{bc} (370 K) and the jump of Δn_{bc} at T_c . The resulting values of a and b and their standard deviations are listed in Table I. Further attempts using higher polynomial expressions did not improve the accuracy of the fit. The reliability of the extrapolation procedure is supported by the good agreement between the Debye temperatures of the specific-heat data at $T > T_3$ and those of the fitted C_p^0 curve in Fig. 2.

III. RESULTS

The excess entropy ΔS of $\text{Pb}_3(\text{PO}_4)_2$ is given as a function of the spontaneous birefringence Δn_{bc} in Fig. 3. The experimental values of Δn_{bc} are taken from Bismayer and Salje.⁷ At temperatures below approximately 415 K we find a strict proportionality

$$-\Delta S = m \Delta n_{bc}, \quad m = 119.653 \pm 0.096, \quad (6)$$

where m is taken in units of cal/mol K. The excess entropy is higher than expected from this relation at temperatures between 415 K and $T_c = 453.6$ K. The difference $-\Delta S - m \Delta n_{bc}$ in Fig. 4 shows clearly a singularity at T_c .

Although the phase transition in $\text{Pb}_3(\text{P}_{1-x}\text{As}_x\text{O}_4)_2$ is continuous only for $x \geq 0.85$, the temperature dependence of ΔC_p near T_c^- can be empirically described by an exponent α for all compositions. The experimental $\ln(\Delta C_p/T)$ vs $\ln t$ curves are shown in Fig. 5 with the reduced temperature $t = |(T - T_1)/T_1|$. The temperature

TABLE I. Values of the transition temperature T_c , the extrapolated upper Curie temperature T_1 , the temperature T_2 of the second peak in the C_p curve, the temperature T_3 where a slight change in the slope of the C_p curve occurs, the value of the latent heat L at the transition point T_c , and the fit parameters a and b of the background specific heat C_p^0 .

	$\text{Pb}_3(\text{PO}_4)_2$	$\text{Pb}_3(\text{P}_{0.97}\text{As}_{0.03}\text{O}_4)_2$	$\text{Pb}_3(\text{P}_{0.2}\text{As}_{0.8}\text{O}_4)_2$
T_c (K)	453.6 ± 0.1	442.3 ± 0.1	424.5 ± 0.1
T_1 (K)	458.5 ± 1	448 ± 1	427 ± 1
T_2 (K)		510 ± 10	490 ± 5
T_3 (K)	530 ± 5	570 ± 5	600 ± 5
L (cal/g)	0.26 ± 0.005	0.24 ± 0.005	0.03 ± 0.005
a (cal/mol K)	84.92 ± 0.20	84.47 ± 0.15	88.25 ± 0.25
b (cal/mol)	-8687 ± 118	-8586 ± 79	-9055 ± 149

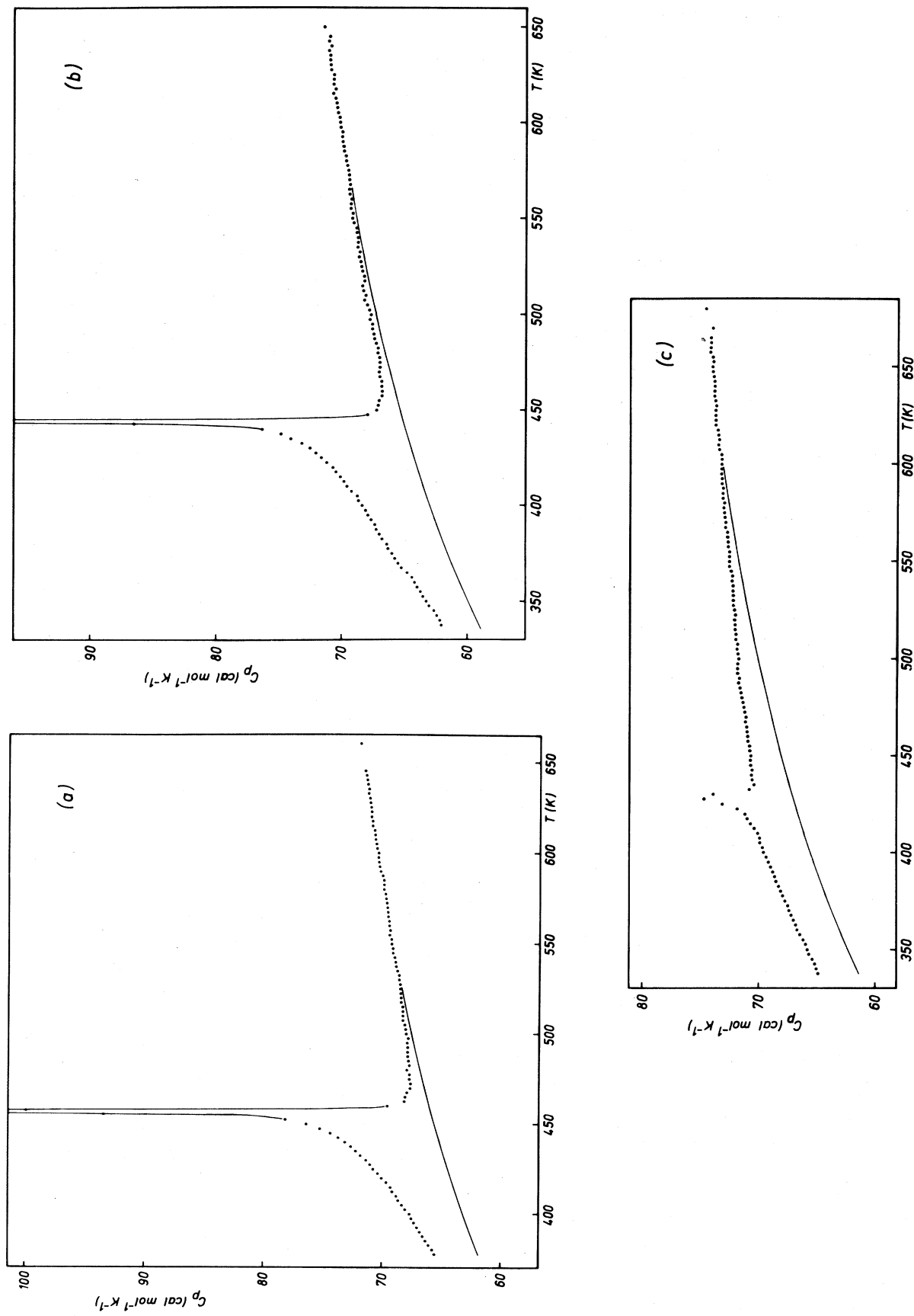


FIG. 1. Temperature dependence of the molar heat capacities of (a) $\text{Pb}_3(\text{PO}_4)_2$, (b) $\text{Pb}_3(\text{P}_{0.97}\text{As}_{0.03}\text{O}_4)_2$, (c) $\text{Pb}_3(\text{P}_{0.2}\text{As}_{0.8}\text{O}_4)_2$. The solid lines at the bottom show the background heat capacities obtained from the analysis by a least-squares fit of Eq. (5). For higher temperatures these curves coincide with the dots representing the measured values.

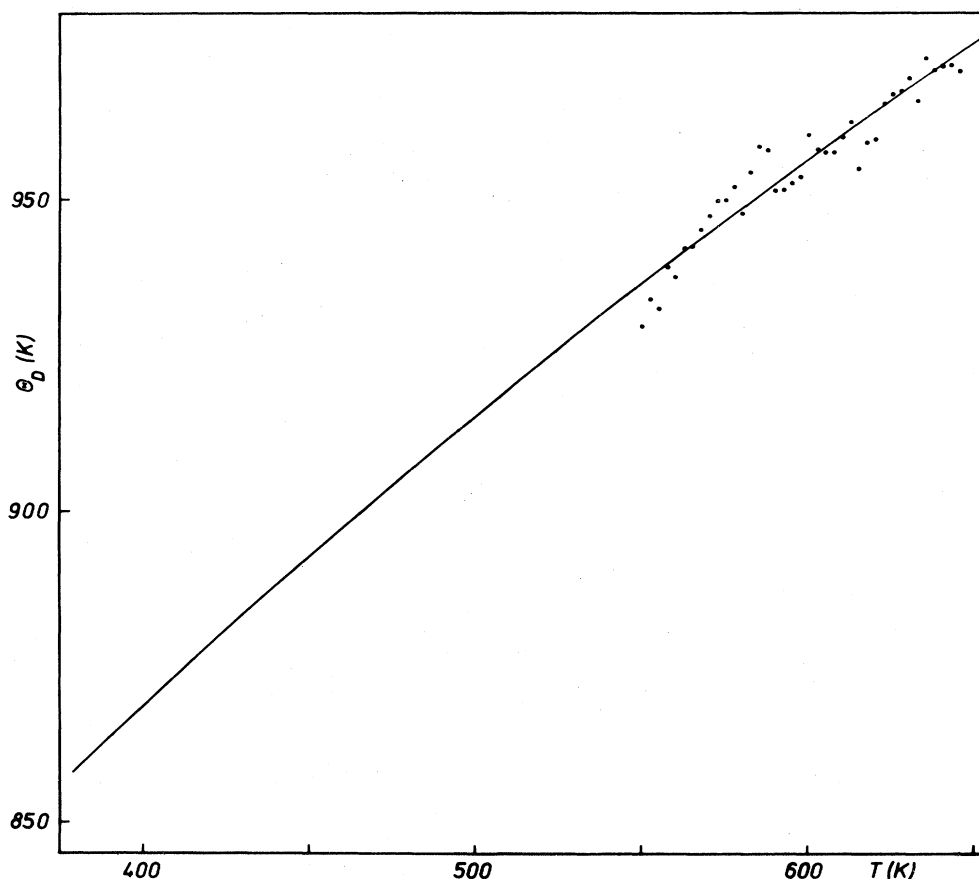


FIG. 2. Debye temperatures Θ_D plotted against T for $\text{Pb}_3(\text{PO}_4)_2$. The dots are calculated from the measured data points, whereas the solid line is obtained from the extrapolated background heat capacity C_p^0 .

$T_1 \geq T_c$ was fitted to give minimum deviation from the proportionality $\ln(\Delta C_p/T) \propto \ln t$. The resulting values of T_1 and the values of T_c are listed in Table I. The experimental exponents α for $T \rightarrow T_c^-$ are 0.363 ± 0.004 for $\text{Pb}_3(\text{PO}_4)_2$, 0.360 ± 0.005 for $\text{Pb}_3(\text{P}_{0.97}\text{As}_{0.03}\text{O}_4)_2$, and 0.36 ± 0.01 for $\text{Pb}_3(\text{P}_{0.2}\text{As}_{0.8}\text{O}_4)_2$. For $T \ll T_c$ the values from Fig. 5 are 0.5 for $\text{Pb}_3(\text{PO}_4)_2$ and 0.0 for $\text{Pb}_3(\text{P}_{0.2}\text{As}_{0.8}\text{O}_4)_2$. The nonanalytic correction for the scaling law

$$C \sim \text{const} |T - T_1|^{-\alpha(1 + a' |T - T_1|^{\Delta_1} + b' |T - T_1| + \dots)}$$

proposed by Adler and Privman¹² when applied in the present calculations did not improve the fit between the experimental data and the theoretical curve.

It is rather surprising that the exponent α appears to be independent of the chemical composition although the order of the phase transition changes. For compounds with high P content the transition is clearly first order, whereas those of compounds with high As content are second order.

Two specific features of the temperature dependence of

the excess specific heat at $T > T_c$ are seen in Fig. 6. First, all compounds shown an extended range of the order of 100 K above T_c with a considerable heat content due to the structural phase transition. The high-temperature limits of these intervals [e.g., 530 K for $\text{Pb}_3(\text{PO}_4)_2$] are at those temperatures where the residual monoclinic splitting of the Raman lines² vanishes.

The second important feature is the appearance of a second peak in the specific-heat curve for the mixed crystals at T_2 (see Table I) but not for pure and stress-free lead phosphate. The temperature T_2 is well defined by a rather sharp peak in the case of $\text{Pb}_3(\text{P}_{0.2}\text{As}_{0.8}\text{O}_4)_2$ but is more difficult to obtain in $\text{Pb}_3(\text{P}_{0.97}\text{As}_{0.03}\text{O}_4)_2$ with a broader cusp in the ΔC_p curve.

IV. DISCUSSION

A. The ferroelastic phase at $T \ll T_c$

The order-parameter dependence of ΔS is given in Eq. (3) and can be directly compared with the spontaneous

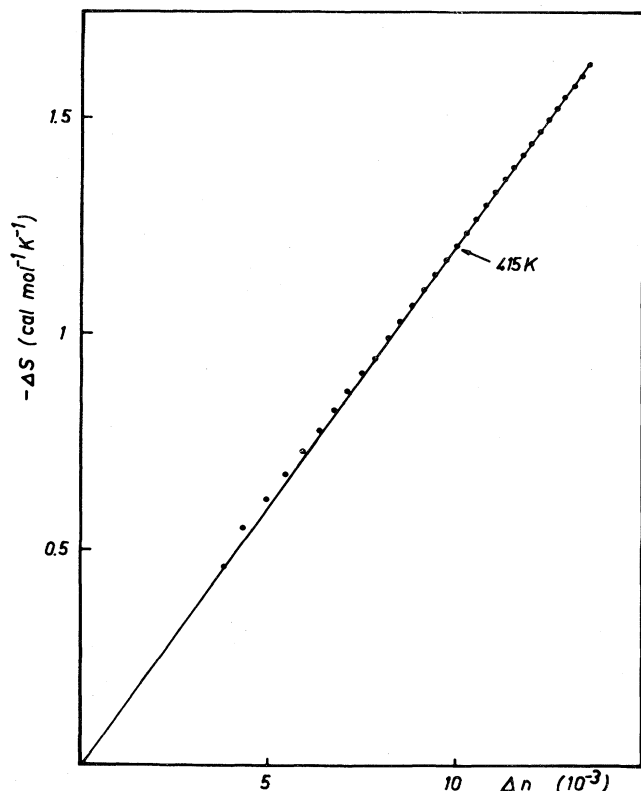


FIG. 3. Entropy ΔS vs birefringence Δn_{bc} for $\text{Pb}_3(\text{PO}_4)_2$ in the temperature range 377.5–453.6 K (T_c).

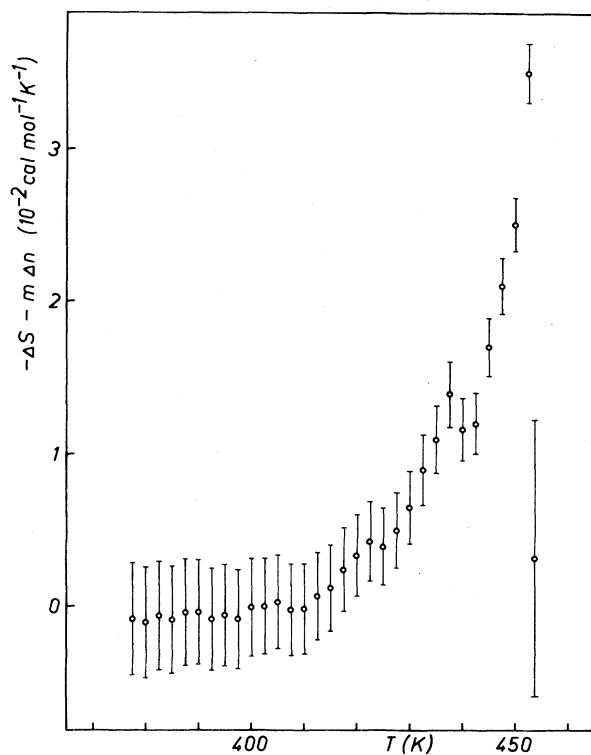


FIG. 4. Difference between the experimental entropy ΔS and the extrapolated values from Eq. (6) for $\text{Pb}_3(\text{PO}_4)_2$.

birefringence Δn_{bc} which is proportional to the ferroelastic strain,⁷ which has been calculated by Salje and Devarajan.⁴ Following their arguments the order-parameter dependence of Δn_{bc} with $Q_2=0$ can be written as

$$\begin{aligned} \Delta n_{bc} &= P_{\text{eff}} e_s \\ &= P_{\text{eff}} (\frac{1}{2} D^2 + 2C^2)^{1/2} (Q_1^2 + 2\sqrt{2} |Q_1 Q_3|), \end{aligned} \quad (7)$$

where P_{eff} is the effective elasto-optic coefficient which has been proved to be temperature independent by Bismayer and Salje.⁷ The constants D and C are defined in Ref. 4. For temperatures far below T_c the two order parameters are proportional with

$$Q_3 = -\frac{1}{\sqrt{2}} Q_1, \quad (8)$$

whereas Q_3 is always larger than $-(1/\sqrt{2})Q_1$ for $T \rightarrow T_c^-$. The difference between both terms is δ with

$$\delta = -\frac{1}{\sqrt{2}} Q_1 - Q_3. \quad (9)$$

The corresponding difference between the optical birefringence and the normalized entropy follows from Eqs. (3), (7), (9):

$$\begin{aligned} \Delta n_{bc} - \frac{3P_{\text{eff}}(\frac{1}{2}D^2 + 2C^2)^{1/2}}{(\alpha_1/2)(1 + \alpha_2/\alpha_1)} |\Delta S| \\ = 2\sqrt{2}P_{\text{eff}}(\frac{1}{2}D^2 + 2C^2)^{1/2} \left[1 - \frac{3}{1 + 2\alpha_1/\alpha_2} \right] Q_1 \delta, \end{aligned} \quad (10)$$

where we have omitted terms of higher order. With $\alpha_2 > \alpha_1$ the left-hand side of Eq. (10) becomes negative as a direct consequence of the multicomponent order-parameter behavior and would vanish in single-component order-parameter theory [$Q_3 \rightarrow (1/\sqrt{2})Q_1$].

The experimentally determined factor m in Eq. (6) is the inverse prefactor of $|\Delta S|$ in Eq. (10),

$$3P_{\text{eff}}(\frac{1}{2}D^2 + 2C^2)^{1/2} \left[\frac{\alpha_1}{2} \left[1 + \frac{\alpha_2}{\alpha_1} \right] \right]^{-1} = \frac{1}{m}.$$

For $T < 415$ K in $\text{Pb}_3(\text{PO}_4)_2$ we find $\Delta n_{bc} \sim |\Delta S|$ and hence $\delta=0$. Close to T_c^- the proportionality between Δn_{bc} and $|\Delta S|$ is broken with $\delta > 0$ based upon differences in the temperature dependence of Q_1 and Q_3 . This proves that Landau theory (at least if only a single one-dimensional order parameter is considered) cannot explain the ferroelastic phase-transition behavior even for $T \lesssim T_c$.

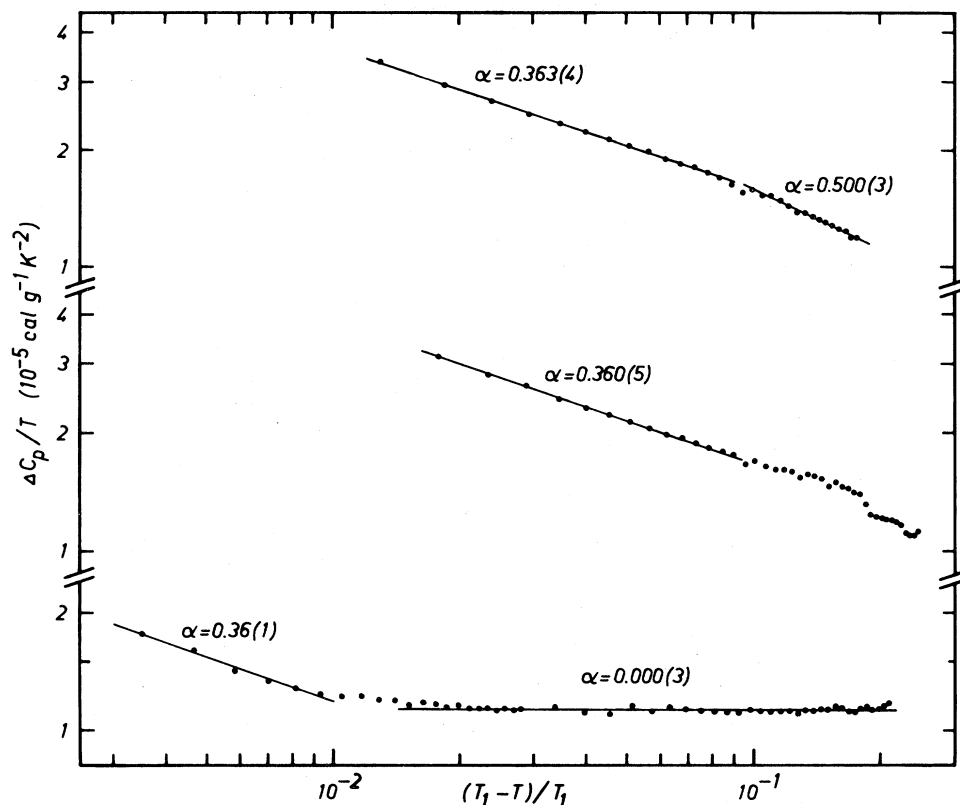


FIG. 5. Plot of the excess specific heats ($T < T_c$) vs the reduced temperature: top curve, $\text{Pb}_3(\text{PO}_4)_2$; middle curve, $\text{Pb}_3(\text{P}_{0.97}\text{As}_{0.03}\text{O}_4)_2$; bottom curve, $\text{Pb}_3(\text{P}_{0.2}\text{As}_{0.8}\text{O}_4)_2$.

B. The exponent α for $T < T_c$

Near T_c^- the value of the specific-heat exponent α depends on the theoretical model adopted for the structural phase transition. It is well known that for a second-order Landau transition a weak (logarithmic) singularity with $\alpha = 0$ occurs. This value was found experimentally for $T \ll T_c$ in $\text{Pb}_3(\text{P}_{0.2}\text{As}_{0.8}\text{O}_4)_2$, the compound which shows an almost continuous phase transition. In the same temperature region, $\text{Pb}_3(\text{PO}_4)_2$ reveals $\alpha = 0.5$ in accordance with a tricritical behavior, where $\alpha = \frac{1}{2}$ follows from the scaling law $\alpha + 2\beta + \gamma = 2$, with $\beta = \frac{1}{4}$ and $\gamma = 1$.

At temperatures very close to T_c^- , the order-disorder phenomena represented by the order parameters Q_1 and Q_2 dominate the phase transition and we expect the α values of the pseudospin Potts model. Theoretical predictions concerning the exponent α are summarized in Table II. Experimentally, all compounds show $\alpha = 0.36$ within experimental error, which is close to the predictions for the $d = 2, q = 3$ Potts transition.

Structurally, the two-dimensional behavior near T_c^- appears plausible from the observation of diffuse neutron and x-ray scattering. Both techniques show cigar-shaped Bragg reflections near T_c^- with the long axis parallel to the trigonal axis.^{2,19} Joffrin *et al.*¹⁹ determined extremely

anisotropic correlation lengths, two longer ones in the $(100)_{\text{mon}}$ cleavage plane and a shorter one perpendicular to the cleavage plane.

TABLE II. Comparison of the critical exponent values α for the ($q = 3$) three-state Potts model with the dimensions $d = 2$ and $d = 3$, respectively.

$q = 3, d = 2$	$\alpha = 0.3365^a$
	0.326^b
	0.320 ± 0.004^c
	0.348 ± 0.008 ($\Delta_1 = 0.56 \pm 0.14$) ^d
	0.331 ± 0.009 ($\Delta_1 = 0.65 \pm 0.12$) ^d
$q = 3, d = 3$	0.35 ± 0.02^e
	$\alpha = 0.5514^a$
	0.5^f
	0.52 ± 0.16^g
	$\alpha' = 0.48 \pm 0.13^g$

^aReference 13.

^bReference 14.

^cReference 15.

^dReference 12.

^eReference 16.

^fReference 17.

^gReference 18.

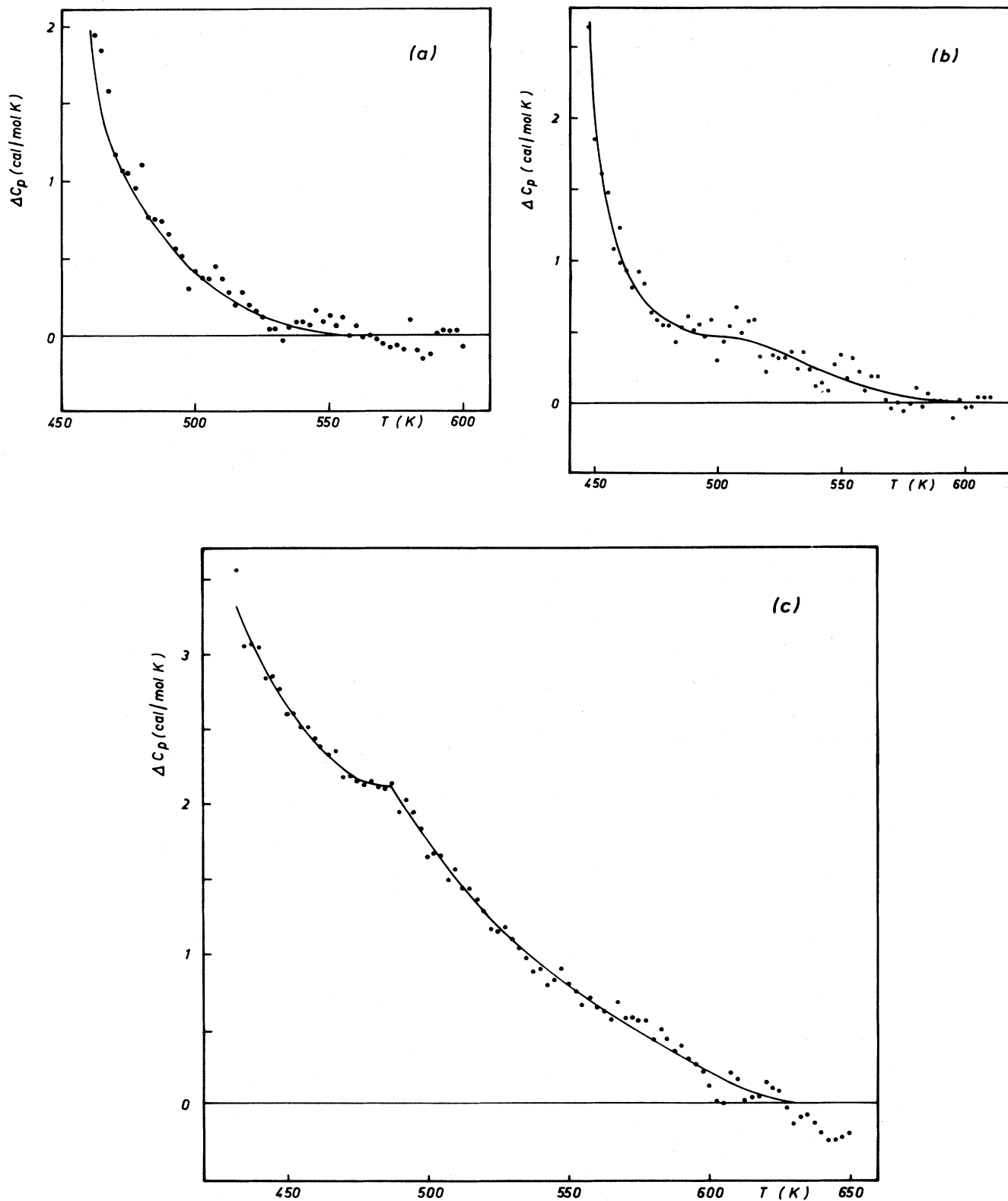


FIG. 6. Excess specific heats in the temperature range $T > T_c$ for (a) $\text{Pb}_3(\text{PO}_4)_2$, (b) $\text{Pb}_3(\text{P}_{0.97}\text{As}_{0.03}\text{O}_4)_2$, (c) $\text{Pb}_3(\text{P}_{0.2}\text{As}_{0.08}\text{O}_4)_2$.

The $d=2$, $q=3$ Potts transition is predicted by most authors to be second order¹²⁻¹⁶ as observed for the As-rich compounds.⁷ The first-order behavior with the same α value for P -rich compounds is probably due to finer details of the transition mechanism closer to T_c than $t \approx 10^{-2}$, where no reproducible C_p values could be measured in this work. Nevertheless, the actual structural transformation, as revealed by all experiments, is essentially the same for all chemical compositions. The order of the phase transition cannot, therefore, be an intrinsic parameter of this type of phase transition.

Theoretically, an alternative explanation for the change of the order of the phase transition results from consideration of the anisotropy parameter $w = \langle Q_3 \rangle$.⁴ The jump at the phase-transition point scales as $w^{0.56}$ (Refs. 5 and 20), so that a second-order transformation appears for $w \rightarrow 0$. This implies that the temperature interval $|T_c^{Q_3} - T_c^{Q_1}|$ is bound to become small for compounds with high As content. From Raman spectroscopic measurements^{2,21} we found this interval to be of the order of 100 K, independent of the chemical composition, which seems to disallow this model.

C. The high-temperature range and the pseudophase a_b

Static or dynamic monoclinic domains have been concluded from results of Raman scattering² for the same temperature interval between T_c and T_3 where excess specific heat is observed. This indicates that the excess specific heat above T_c is due to two contributions: the ferroelastic phase transition and the structural deformation due to monoclinic precursor effects. The determination of the exponent α for $T \rightarrow T_c^+$ therefore encounters the typical difficulty due to precursor ordering effects.²² Furthermore, the fluctuations originate from the three independent order parameters Q_1 , Q_2 , and Q_3 , which implies a superposition of fluctuations of Pb atoms perpendicular to the trigonal axis (Q_3) and fluctuations from the rotations around the trigonal axis (Q_1, Q_2), the so-called flip motion.⁴ Hence, an unequivocal interpretation of the specific heat only in terms of fluctuations of one single type does not appear to be possible. As a first approach, we tried to fit the experimental data points with a scaling law $\Delta C \sim t^{-\alpha}$ and, alternatively, with a soft-mode behavior of the type

$$\omega^2 \sim A(T - T_c) + Bq^2 \quad (11)$$

which gives the related form²³

$$\Delta C \sim T^2 \ln \frac{1}{|T - T_c|} \quad (12)$$

As in the case of potassium dihydrogen phosphate²² (KDP), we find a rather poor fit for the scaling law with a critical exponent near 1.0. The logarithmic singularity with $\alpha \rightarrow 0$ is, on the other hand, in much better agreement with our experimental results. In Fig. 7 the excess specific heat of $\text{Pb}_3(\text{PO}_4)_2$ is plotted against $\ln t$, showing a good fit in the temperature range from 465 to 530 K. Assuming a logarithmic divergence, the critical region encountered in

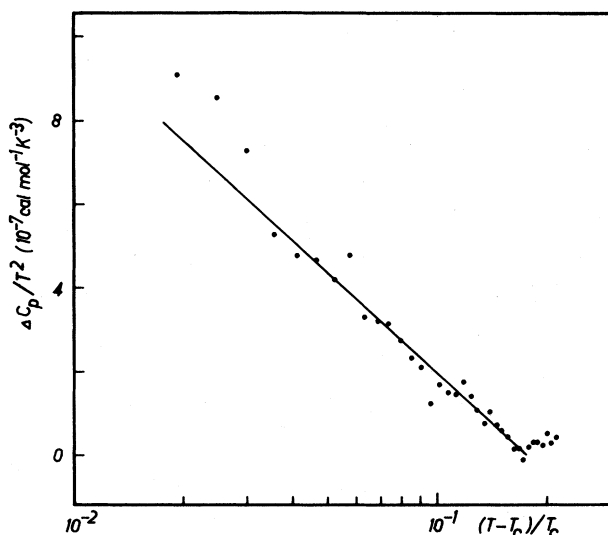


FIG. 7. $\Delta C_p/T^2$ vs $|T - T_c|/T_c$ for $\text{Pb}_3(\text{PO}_4)_2$ at $T > T_c$.

$\text{Pb}_3(\text{PO}_4)_2$, as evidenced by the region of fit to the assumed divergence, is surprisingly large. This may be taken as an indication that the influence of the precursor ordering as well as the Q_3 fluctuations is much smaller than that of the flip-mode fluctuations. Nevertheless, the much better fit of the excess specific heat to a power law instead of a logarithmic singularity for $T \rightarrow T_c^-$ reveals an asymmetric thermodynamic behavior with respect to $T_c^+ = T_c^-$, which is in strict contradiction to the scaling laws. We therefore prefer to think of the specific heat for $T > T_c$ as a superposition of the above-mentioned processes and the observed logarithmic singularity as an empirical fit of the experimental data points. Further Raman spectroscopic experiments on the role of the precursor ordering are under way and may give additional information to disentangle the different contributions to the excess specific heat.

The second important feature is the appearance of a small peak in the specific-heat curve at T_2 for mixed crystals but not for $\text{Pb}_3(\text{PO}_4)_2$. The temperature T_2 has also been found in x-ray experiments² where the temperature interval between T_c and T_2 [nonexistent for pure $\text{Pb}_3(\text{PO}_4)_2$ because $T_c = T_2$] is characterized by static monoclinic deformations in a trigonal matrix. In agreement with results from neutron scattering,¹⁹ the diffuse x-ray scattering above T_2 is identified as dynamical scattering from the lowest-energy phonon branches²⁴ and the effect of the flip mode.² The observed peaks at T_2 , therefore, indicate the crossover points from the static regime of the crystallographic phase a_b to the dynamic regime at higher temperatures.

The present results thereby confirm earlier observations that no static intermediate phase exists for pure, stress-free $\text{Pb}_3(\text{PO}_4)_2$ but is immediately induced by dopants [here As in $\text{Pb}_3(\text{P}_{0.97}\text{As}_{0.03}\text{O}_4)_2$] or even external strain.² The observation of a static intermediate phase for the mixed crystals

is also in agreement with results of neutron scattering,^{25,26} where no central peak was found for $\text{Pb}_3(\text{PO}_4)_2$ but was found for vanadium-doped crystals.

The only contradictory experimental results are those of electron microscopy published recently by Torrès *et al.*,²⁷ where the authors claim to have observed a "ferroelastic" phase a_b in $\text{Pb}_3(\text{PO}_4)_2$. Nevertheless, the ferroelastic strain is a macroscopic quantity and was clearly found to vanish just above T_c .^{3,7,28} It seems probable from the present results that further strain components are induced during the preparation of extremely thin probes by ion-bombardment and that the static monoclinic structural deformation is stabilized by strain effects.

The origin of the peak at T_2 depends on the structural model assumed for the intermediate phase a_b . Two models have been discussed in the past: Torrès and Aubree²⁹ proposed a monoclinic, pseudotrigonal structure with eight formula units per crystallographic unit cell,

whereas Joffrin *et al.*³⁰ and Bismayer *et al.*² showed that the assumption of quasistatic monoclinic microdomains also explains the experimental findings. In the second case the correlation between these microdomains is not yet understood and experimental work is in progress to solve the crystal structure of the a_b phase. In any case, at T_2 we find a structural phase transition between the crystallographic phase a_b and the trigonal phase a . The small cusp in the specific heat at T_2 may, therefore, be indicative of a slightly first-order effect of this phase transition, or it may be due to impurities as recently discussed by Scott *et al.*³¹ for BaMnF_4 .

ACKNOWLEDGMENTS

We are thankful to Dr. Devarajan for fruitful discussions. The project was supported by the German Science Foundation (Sa-245/7-1).

¹J. Torrès, Phys. Status Solidi B **71**, 141 (1975).

²U. Bismayer, E. Salje, and C. Joffrin, J. Phys. (Paris) **43**, 1379 (1982).

³I. G. Wood, V. K. Wadhawan, and A. M. Glazer, J. Phys. C **13**, 5155 (1980).

⁴E. Salje and V. Devarajan, J. Phys. C **14**, L1029 (1981).

⁵A. Aharony, K. A. Müller, and W. Berlinger, Phys. Rev. Lett. **38**, 33 (1977).

⁶R. B. Potts, Proc. Cambridge Philos. Soc. **48**, 106 (1952).

⁷U. Bismayer and E. Salje, Acta Crystallogr. Sect. A **37**, 145 (1981).

⁸M. Chabin, F. Gilletta, and J. P. Ildefonse, J. Appl. Crystallogr. **10**, 247 (1977).

⁹M. J. O'Neill, Anal. Chem. **38**, 1331 (1966).

¹⁰D. C. Ginnings and G. T. Furukawa, J. Am. Chem. Soc. **75**, 522 (1953).

¹¹F. Gilletta, M. Chabin, and Cao Xuan An, Phys. Status Solidi A **35**, 545 (1976).

¹²J. Adler and V. Privman, J. Phys. A **15**, L417 (1982).

¹³T. W. Burkhardt, H. J. F. Knops, and M. P. M. den Nijs, J. Phys. A **9**, L179 (1976).

¹⁴C. Dasgupta, Phys. Rev. B **15**, 3460 (1977).

¹⁵S. Elitzur, R. B. Pearson, and J. Shigemitsu, Phys. Rev. D **19**, 3698 (1979).

¹⁶M. Bretz, Phys. Rev. Lett. **38**, 501 (1977).

¹⁷E. K. Riedel and F. J. Wegner, Phys. Rev. Lett. **29**, 349 (1972).

¹⁸H. J. Herrmann, Z. Phys. B **35**, 171 (1979).

¹⁹C. Joffrin, M. Lambert, and G. Pepy, Solid State Commun. **21**, 853 (1977).

²⁰G. R. Golner, Phys. Rev. B **8**, 3419 (1973).

²¹E. Salje and U. Bismayer, Phase Trans. **2**, 15 (1981).

²²W. Reese and L. F. May, Phys. Rev. **162**, 510 (1967).

²³A. Y. A. Gordon, Phys. Status Solidi B **87**, K57 (1978).

²⁴C. Joffrin, J. P. Benoit, R. Currat, and M. Lambert, J. Phys. (Paris) **40**, 1185 (1979).

²⁵J. P. Benoit, B. Hennion, and M. Lambert, Phase Trans. **2**, 102 (1981).

²⁶J. Torrès and C. Joffrin, Ferroelectrics **26**, 665 (1980).

²⁷J. Torrès, C. Roucau, and R. Ayroles, Phys. Status Solidi A **70**, 659 (1982).

²⁸D. M. C. Guimaraes, Phase Trans. **1**, 143 (1979).

²⁹J. Torrès, and J. Aubree, Ferroelectrics **21**, 589 (1978).

³⁰C. Joffrin, J. P. Benoit, L. Deschamps, and M. Lambert, J. Phys. (Paris) **38**, 205 (1977).

³¹J. F. Scott, F. Habbal, and M. Hidaka, Phys. Rev. B **25**, 1805 (1982).